Lysosome and HER3 (ErbB3) Selective Anticancer Agent Kahalalide F: Semisynthetic Modifications and Antifungal Lead-Exploration Studies

Abbas Gholipour Shilabin,[†] Noer Kasanah,[†] David E. Wedge,[‡] and Mark T. Hamann*,[†]

Department of Pharmacognosy, School of Pharmacy, The University of Mississippi, University, Mississippi 38677, and USDA-ARS, Natural Product Utilization Research Unit, National Center for Natural Products Research, University of Mississippi, University, Mississippi 38677

Kahalalide F (**1**) shows remarkable antitumor activity against different carcinomas and has recently completed phase I clinical trials and is being evaluated in phase II clinical studies. The antifungal activity of this molecule has not been thoroughly investigated. In this report, we focused on acetylation and oxidation of the secondary alcohol of threonine, as well as reductive alkylation of the primary amine of ornithine, and each product was evaluated for improvements in antifungal activity. **1** and analogues do not exhibit antimalarial, antileishmania, or antibacterial activity; however, the antifungal activity against different strains of fungi was particularly significant. This series of compounds was highly active against *Fusarium* spp., which represents an opportunistic infection in humans and plants. The in vitro cytotoxicity for the new analogues of **1** was evaluated in the NCI 60 cell panel. Analogue **5** exhibited enhanced potency in several human cancer cell lines relative to **1**.

Introduction

The kahalalides are a family of natural depsipeptides that were first isolated from the Hawaiian herbivorous marine sacoglossan mollusk *Elysia rufescens* (Plakobranchidae) and later from its green algal diet of *Bryopsis pennata* (Bryopsidaceae).[1−8] Kahalalide F (KF,[a] **1**) is the largest and most biologically active cyclic peptide of the 13 natural peptides isolated from *E. rufescens*. Kahalalides are likely secondary metabolites synthesized by an associated microorganism or from the diet of the green algae *B. pennata*. **1** is a tridecapeptide with the molecular formula $C_{75}H_{124}N_{14}O_{16}$ and mass 1477.9408 $[M + H]^+$ composed of a cyclized macrolide region and a linear region with a 5-methylhexanoic acid, conjugated with the N-terminus. Investigations of the structure of **1** revealed a NRPS peptide (*cyclo*[L-Val(1)-Z-Dhb-L-Phe-D-Val(2)-D-*allo*-Ileu(1)-D-*allo*-Thr-(1)]-D-*allo*-Ileu(2)-L-Orn-D-Pro-D-Val-(3)-L-Val(4)-L-Thr(2)-D-Val(5)-5-MeHex) (Figure 1).[1,9,10]

1 exhibits significant in vitro and in vivo antitumor activity in various solid tumor models, including colon (HT-29), breast (T-47D), non-small-cell lung (A-549), and prostate cancer (DU-145). The activity of **1** has been investigated in phase I clinical trials for androgen-refractory prostate cancer[11] and in phase II clinical studies with patients having liver cancer, non-small-lung cell cancer (NSCLC), and melanoma.[12] Recently, the results of the phase II clinical study of kahalalide F in patients with advanced NSCLC, hepatocarcinoma (HC), and advanced malignant melanoma (AMM) have been reported at the 31st European Society for Medical Oncology Congress (ESMO), revealing an excellent tolerability profile with no serious adverse events.[13] A positive response and stable disease were observed in a number of patients.
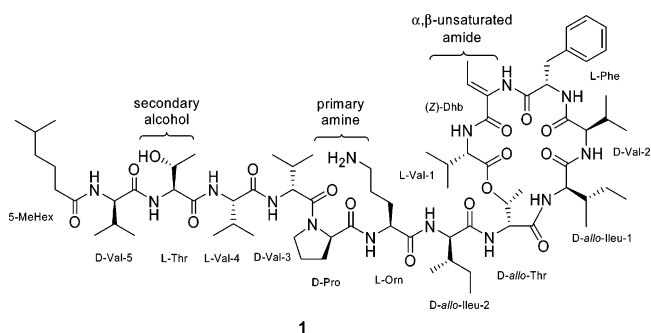

Figure 1. Kahalalide F and target functional groups for synthetic modification and lead optimization.

Lysosomes are intracellular targets of **1**. Treatment of tumor cells with **1** resulted in larger vacuoles, and target cells became dramatically swollen because of changes in lysosomal membrane.[14] Further investigations consistently showed the loss of lysosomal integrity and the induction of cytoplasmic swelling and vacuolization in breast and prostate cancer cells.[15] More recent studies have suggested that inhibition of the HER/neu (ErbB) family signaling is a part of the mechanism of kahalalide F's action.[16] The cytotoxic activity of **1** against several tumor types significantly correlated with protein expression levels of the ErbB3 receptor.[17] This specific interaction has been described in a translational program that has confirmed a selective down-regulation of ErbB3 expression by **1** treatment. These findings suggest that ErbB3 may be a potential determinant for **1** sensitivity in patients.[18] Trastuzumab (145K amu protein), is a humanized monoclonal antibody that acts on the HER2/neu (ErbB2) receptors. Recently, trastuzumab was used in the treatment of HER2-positive metastatic breast cancer as an anticancer therapy. It is believed that in patients whose tumors overexpress HER2 receptors, trastuzumab can turn off HER2−HER2 homodimers. Unlike available marketed drugs for HER1 (cetuximab [146K amu protein], gefitinib [*N*-(3-ethynylphenyl)-6,7-bis(2-methoxyethoxy)quinazolin-4-amine], and erlotinib [*N*-(3-chloro-4-fluorophenyl)-7-methoxy-6-(3-morpholin-4-ylpropoxy)-quinazolin-4-amine]), and HER2 (trastuzumab) related cancers, there is no report regarding HER3 (ErbB3) inhibiting drugs.[19]

---

* To whom correspondence should be addressed. Telephone: 662-915-5730. Fax: 662-915-6975. E-mail: mthamann@olemiss.edu.

† School of Pharmacy.

‡ USDA-ARS, National Center for Natural Products Research.

a Abbreviations: KF, kahalalide F; KG, kahalalide G; KD, kahalalide D; SAR, structure−activity relationship; NSCLC, non-small-cell lung cancer; HC, hepatocarcinoma; AMM, advanced malignant melanoma; CNS, central nervous system; FS, fungistatic; FC, fungicidal; MABA, microplate Alamar blue assay; RMP, rifampcin; Amp B, amphotericin B; Capt, captan; azoxy, azoxystrobin.

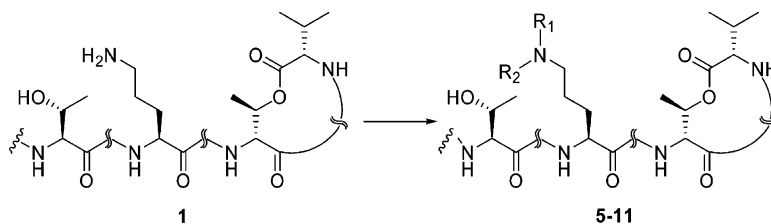**Scheme 1.** Hydrolysis of Kahalalide F to Kahalalide G[a]
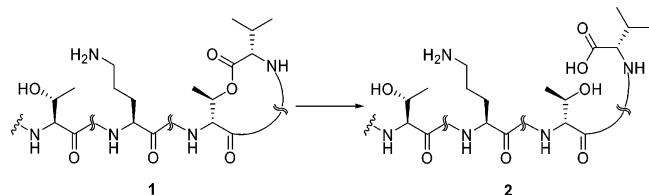
a Reagents and conditions: K2CO3, H2O/MeOH (1:2), room temp, 8 h, 95%.

Scheme 2. Conversion of **1** to the Acetate and Oxo Analogues[a]
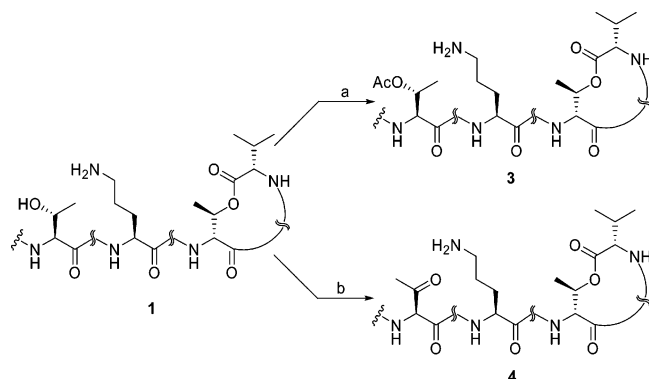
a Reagents and conditions: (a) Ac2O, BF3·OEt2, CH2Cl2, room temp, 5 min, 68%; (b) Dess–Martin periodinane (DMP), MeCN, room temp, 1 h, 75%.

As a result, **1** and its anologues would be promising candidates for inhibition of HER3 receptors in tumor cells. The mechanism of action of **1** on fungi may involve targets similar to the human tumor cells.

Because of the limited availability of the natural product, data regarding structure−activity relationship (SAR) studies of **1** have not been reported in the literature and remain limited to the data generated from isolated natural products, as well as solid-phase total synthesis reported for **1**.[10,20−22] In a continued investigation of biologically active marine natural products and

their optimization using semisynthesis, we were particularly interested in structure−activity relationships of **1** analogues against opportunistic fungal infections of humans and plants.[23−25]

In this study we focused our attention on the secondary alcohol of threonine and the primary amine of ornithine as the key functional groups for modification beginning with the natural product because they play a crucial role in the bioactivity of this class of compounds.[26] Additional semisynthetic modifications and biocatalytic studies will be evaluated in due course.[21]

We evaluated the activity of the parent compound and its derivatives for antiprotozoal, antibacterial, and antifungal activity focusing on *Fusarium* spp. because of the challenge of treating these opportunistic infectious diseases.[27] Immunocompromised patients with invasive fungal infections have increased in recent decades because of a greater number of transplant patients, more aggressive anticancer chemotherapeutic regimens, and the emergence of AIDS. The therapeutic interventions for fungal infections are limited. The most commonly encountered etiologic agents of systemic fungal infections in immunocompromised patients are *Candida* spp., *Aspergillus* sp., *Cryptococcus neo-formans*, *Fusarium* spp., and *Trichosporon* spp.[28] We focused our attention on the SAR of **1** against fungal infections caused by *Fusarium* spp. because there are a limited number of drugs active against these fungi. It is also noteworthy that peptides are a well established source of antibiotics including gramicidins, polymyxins, bacitracins, vancomycin, teicoplanin, and echi-nocandins.[29] However, among these only the echinocandin family is active against fungi and is a noncompetitive inhibitor of the synthesis of 1,3-β-D-glucan, a major component of the fungal cell wall.[30]

Results and Discussion

1. Semisynthesis of Kahalalide F Analogues. For spectro-scopic and biological comparison, we first converted **1** to kahalalide G (KG, **2**) under mild basic conditions. This reaction also provided valuable information regarding stability of the lactone under basic conditions. Kahalalide F was hydrolyzed

Scheme 3. Synthesis of Monoalkyl and Dialkyl N-Substituted KF Based on Stepwise Reductive Alkylation in the Presence of a Carboxaldehyde and Triacetoxyborohydride[a]

Compound	R1	R2	Yield (%)
4-Fluro-benzylamino-KF (**5**)	H	benzyl-F	64.5
Bis(4-fluoro-benzyl)amino-KF (**6**)	benzyl-F	benzyl-F	3.1
4-Pyridinylmethylamino-KF (**7**)	H	pyridinyl-N	53.1
2-Thienylmethylamino-KF (**8**)	H	thienyl-S	52.3
Bis(2-thienylmethyl)amino-KF (**9**)	thienyl-S	thienyl-S-CH3	12.6
n-Hexylamino-KF (**10**)	H	CH3	45.1
Bis(*n*-hexyl)amino-KF (**11**)	CH3	CH3	25.3

a Reagents and conditions: aldehydes, Na(OAc)3BH, MeOH, 3 Å molecular sieves, room temp.

at the ester linkage using H_2O–MeOH (2:1) in the presence of potassium carbonate at room temperature affording cleavage of the macrolactone to the target ring-opened product **2** (Scheme 1).

Our studies continued with the acetylation of kahalalide F. Ramirez et al. reported that the complete acetylation of a vast array of secondary and tertiary alcohols could be readily achieved by treatment with acetic anhydride and $BF_3 \cdot OEt_2$ at room temperature for a just few seconds.[31] However, without control of the reaction time, the formation of an array of acetate species occurred.

Treatment of **1** free base with an excess 2:1 volumetric ratio of acetic anhydride to $BF_3 \cdot OEt_2$ at room temperature after 5 min afforded KF monoacetate (**3**) with a 68% yield (Scheme 2). Compound **3** showed a molecular $[M + H]^+$ ion peak at *m/z* 1519.9478 in high-resolution electrospray ionization mass spectrometry (HRESIMS) in positive mode. ^{1}H NMR of the monoacetate **3** shows that the β-proton of L-threonine shifted downfield to 5.00 ppm. This signal along with the β-proton of D-*allo*-threonine at 5.04 ppm suggested two ester linkages, which were validated by heteronuclear multiple-bond correlation (HMBC) between β-protons of L-threonine and D-*allo*-threonine with the corresponding carbonyl groups of acetyl at 169.9 ppm and L-Val-1 at 169.8 ppm, respectively. Further confirmation of O-acetylation was secured by the observation of HMBC correlation between the new carbonyl signal at 169.9 ppm and the methyl singlet at 1.92 ppm.

The addition of the Dess–Martin periodinane (DMP)[32] to a solution of **1** in acetonitrile furnished the oxidation of the secondary alcohol to the corresponding oxo-KF (**4**) in good yield (75%). The presence of a trace amount of an unknown byproduct was observed during repeated HPLC purification, likely due to the reversible formation of a Schiff's base between the new carbonyl and the NH_2 of ornithine. High-resolution TOF-ESI-MS of analogue **4** provided molecular mass of $[M + H]^+$ at *m/z* 1475.9237, corresponding to the loss of 2 mass units, in comparison with parent molecule. The presence of a $C{=}O$ resonance at 200.9 ppm in the ^{13}C NMR spectrum and elimination of the CH–OH signal at 66.9 ppm from the **1** spectrum in ^{13}C NMR and DEPT 135° (distortionless enhancement by polarization transfer, 135°) spectra unambiguously revealed the oxidation of the secondary alcohol of threonine to a ketone group. Furthermore, the loss of the OH singlet and associated methine CH–OH in the ^{1}H NMR provides additional evidence for this transformation.

To gain a better understanding of the structure–activity relationships of **1**, we extended the range of **1** derivatives by alkylating the primary amine group of the L-ornithine residue. Synthetic approaches were based on the stepwise reductive N-alkylation of the amino group to the corresponding monoalkyl- or dialkylamino-KF in the presence of a carboxaldehyde and hydride reducing agent.[33,34] This stepwise one-pot procedure involves the initial formation of the intermediate carbinol amine, which dehydrates to form an imine. Subsequent in situ reduction of this imine produces the alkylated amine. The reductive alkylation of **1** with aldehydes was best performed under optimized conditions in which the parent molecule was exposed to 5 equiv of aldehyde in methanol for 30 min at room temperature prior to portionwise addition of 2 equiv of sodium triacetoxyborohydride [$NaBH(OAc)_3$] at the same conditions. The reaction time was varied from a few hours to a couple of days and gave the desired products in good yields; however, the formation of dialkylated amines in low yield was found to be a common side reaction (Scheme 3).
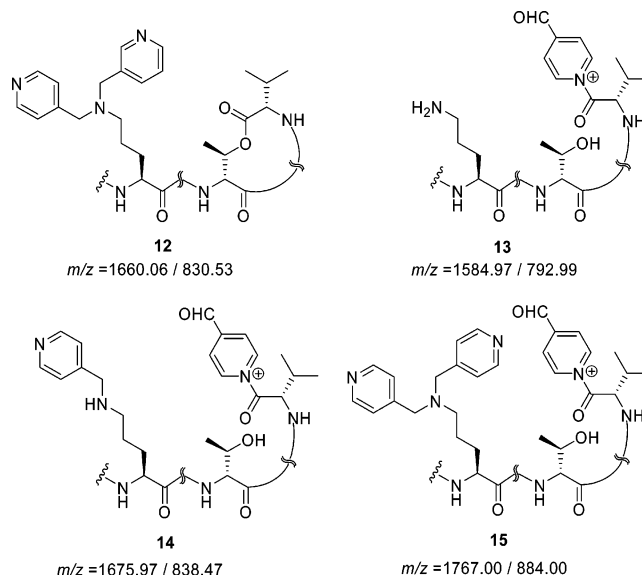

Figure 2. Byproducts resulting from reductive alkylation of **1** and 4-pyridinecarboxaldehyde detected by LC–MS (single charge/double charges unit mass).
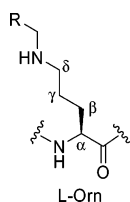
Attempts to accomplish a similar reductive alkylation reaction in the presence of 4-pyridinecarboxaldehyde resulted in a lower yield of 4-pyridinylmethylamino-KF (**7**) and bis(4-pyridinylmethyl)amino-KF (**12**) relative to other alkylamino derivatives. We were not able to isolate trace amounts of the dialkylamine moiety. Because of the basic nature of 4-pyridinecarboxaldehyde, the cyclic macrolactone appears to be attacked by this base to give an opened-ring species (**13**–**15**), which are detectable only with LC–MS (Figure 2).

In order to protect the parent molecule from further basic ring-opening reactions and formation of undesired byproducts, preliminary stirring of the reaction mixture was eliminated for the reductive alkylation of **1** using 4-pyridinecarboxaldehyde and morpholin-4-ylbenzaldehyde.

The structures of N-alkylated KF analogues were confirmed with spectroscopic (^{1}H NMR and DEPT 135°) and high-resolution ESIMS techniques (Table 1 and Supporting Information).

To understand the kinetics and distribution of **1** by fluorescence microscopy, a coumarin-based fluorophore of **1** was prepared through an amidation reaction.[35] As shown in Scheme 4, the target fluorescent molecule was synthesized by treatment of DEAC-carboxylic acid and **1** in the presence of EDC and HBTU in DMF at room temperature for 1 h. In this reaction, the primary amine reacted with high chemo- and regioselectivity in the presence of the secondary alcohol and amides giving exclusively the desired DEAC-KF-amide (**16**) as an intense yellow solid in good yield.

Compound **16** showed a molecular $[M + H]^+$ ion peak at *m/z* 1721.0282 in HRESIMS. Three additional aromatic protons of this analogue at 6.61 (s, 1H), 6.77 (m, 1H), and 7.67 (m, 1 H) ppm in ^{1}H NMR spectrum along with a chemical shift at 3.48 (m, 4H) ppm for two methylene groups and a characteristic signal at 8.66 (s, 1H) ppm assignable to the 2-pyrone moiety revealed the formation of a new amide linkage between DEAC acid and **1**. Further validation of the structure was obtained from the DEPT 135° spectrum at 12.8 ($2 \times CH_3$), 44.8 ($2 \times CH_2$), 96.4 (Ph), 110.6 (Ph), 132.0 (Ph), 148.2 (pyrone) ppm.

Table 1. Selected ^{1}H NMR and DEPT 135° Data for **1** and Its N-Alkylated KF Analogues in DMSO-$d_6{}^a$

L-Orn

		^{1}H NMR			^{13}C NMR		
		L-ornithine		derivative (R)	L-ornithine		derivative (R)
compd	HRESIMS [M + H]$^+$	NHR	CH_2(δ)	residue	CH_2(δ)	NHCH$_2$R	Residue
1	1477.9408	7.62 (m, 2H, NH$_2$)	2.74 (m)	7.19−7.28 (m, 5H, Ph)	38.7		126.8 (Ph), 128.5 (2C, Ph), 129.5 (Ph), 130.1 (Ph)
5	1585.9769	7.60 (m)	2.91 (m)	7.18−7.28 (m, 5H, Ph), 7.49−7.52 (m, 2H, Ph), 8.77−8.80 (m, 2H, Ph)	38.5	46.6	115.9 (Ph), 116.1 (Ph), 127.0 (Ph), 128.6 (2C, Ph), 129.7 (Ph), 130.3 (Ph), 132.7 (Ph), 132.8 (Ph)
7	1568.9814	7.63 (m)	2.93 (m)	7.21−7.28 (m, 5H, Ph), 7.49 (m, 2H, Py), 8.66 (s, 2H, Py)	38.5	47.6	124.7 (2C, Py), 126.9 (Ph), 128.7 (2C, Ph), 129.7 (Ph), 130.3 (Ph), 150.3 (2C, Py)
8	1573.9429	7.63 (m)	2.92 (m)	7.22−7.29 (m, 5H, Ph), 7.10 (m, Th), 7.21 (m, Th), 7.57 (m, Th)	38.5	47.6	126.9 (Ph), 127.8 (Th), 128.6 (2C, Ph), 128.7 (Th), 129.7 (Ph), 130.2 (Ph), 130.9 (Th)
10	1562.0334	7.59 (m)	2.85 (bs)	7.21−7.27 (m, 5H, Ph), 0.61−1.55 (m, 13H, aliphatic)	38.5	47.6	14.3 (CH$_3$), 22.3 (CH$_2$), 25.8 (CH$_2$), 26.0 (CH$_2$), 31.1 (CH$_2$), 126.9 (Ph), 128.6 (2C, Ph), 129.7 (Ph), 130.2 (Ph)
11	1646.1271		2.95 (bs)	7.18−7.25 (m, 5H, Ph), 0.61−1.55 (m, 26H, aliphatic)	38.4	47.6	14.3 (CH$_3$), 22.4 (CH$_2$), 23.4 (CH$_2$), 23.5 (CH$_2$), 31.2 (CH$_2$), 127.0 (Ph), 128.6 (2C, Ph), 129.7 (Ph), 130.2 (Ph)

^{a} Abbreviations: Ph = phenyl, Py = pyridine, Th = thienyl.

Scheme 4. Amidation Reaction of Kahalalide F and DEAC Acid in the Presence of a Coupling Agent^a
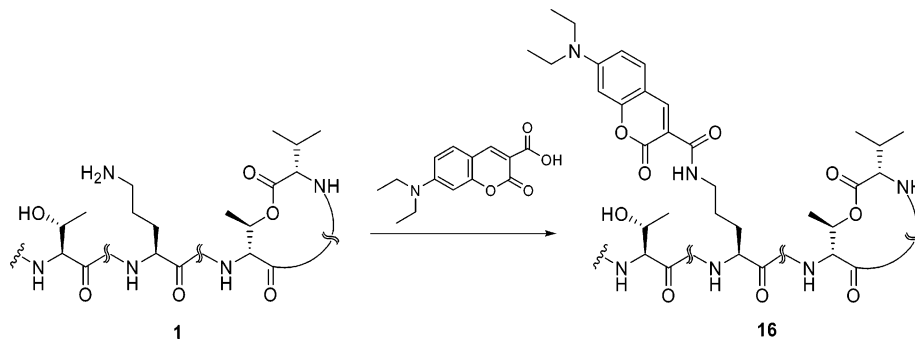
^{a} Reagents and conditions: *O*-(benzotriazol-1-yl)-*N,N,N′,N′*-tetramethyluronium hexafluorophosphate (HBTU), *N*-ethyl-*N′*-(3-dimethylaminopropyl)carbodiimide (EDC), DMF, room temp, 1 h, 84.9%.

Table 2. In Vitro Data of Antimicrobial Activities[a]

compd	*C. albicans* ATCC 90028 (μM)			*C. neoformans* ATCC 90113 (μM)			*A. fumigatus* ATCC 90906 (μM)			*M. intracellulare* ATCC 23068 (μM)		
	IC_{50}	MIC	MFC	IC_{50}	MIC	MFC	IC_{50}	MIC	MFC	IC_{50}	MIC	MBC
1	3.02 ± 0.04	10	20	1.53 ± 0.38	5	5	3.21 ± 0.05	10	20	>20	>20	>20
2	>13.38	NT	NT	>13.38	NT	NT	>13.38	NT	NT	>13.38	NT	NT
KD	>33.57	NT	NT	>33.57	NT	NT	>33.57	NT	NT	>33.57	NT	NT
3	3.28 ± 0.02	10	20	1.89 ± 0.01	5	5	3.38 ± 0.09	10	10	14.32 ± 0.33	>20	>20
4	12.44 ± 0.07	>20	>20	4.34 ± 0.44	10	20	>13.6	>20	>20	>20	>20	>20
5	>12.6	>20	>20	3.77 ± 0.09	10	10	>12.6	>20	>20	>20	>20	>20
6	>11.81	NT	NT	>11.81	NT	NT	>11.81	NT	NT	>11.81	NT	NT
7	4.19 ± 0.11	>20	>20	2.12 ± 0.37	5	5	4.26 ± 0.1	10	20	>20	>20	>20
8	3.81 ± 0.14	10	20	1.91 ± 0.23	5	10	3.22 ± 0.06	10	20	11.98 ± 0.57	>20	>20
10	5.69 ± 0.15	20	20	1.93 ± 0.07	5	10	3.12 ± 0.02	10	20	>20	>20	>20
11	>12.2	>20	>20	6.71 ± 0.02	>20	>20	>12.2	>20	>20	>20	>20	>20
16	>11.62	NT	NT	>11.62	NT	NT	>11.62	NT	NT	>11.62	NT	NT
amphotericin B	0.25 ± 0.04	0.625	1.25	0.79 ± 0.05	0.016	0.06	1.32 ± 0.06	2.5	2.5	NT	NT	NT
ciprofloxacin	NT	NT	NT	NT	NT	NT	NT	NT	NT	0.42 ± 0.07	1.0	>1

[a] NT = not tested. Amphotericin B (a polyene antifungal drug) and ciprofloxacin (1-cyclopropyl-6-fluoro-4-oxo-7-piperazin-1-ylquinoline-3-carboxylic acid) are used as positive antifungal and antibacterial controls, respectively. The IC_{50} is the concentration that affords 50% inhibition of growth. MIC (minimum inhibitory concentration) is the lowest test concentration that yields detectable growth. MFC/MBC (minimum fungicidal/bactericidal concentration) is the lowest test concentration that kills 100% of the organism.

2. Biological Evaluation of Products. 2.A. Activity in Opportunistic Infections. Kahalalide D (KD), **2**, **1**, and its analogues were evaluated in vitro for their activity against several microorganisms that cause opportunistic infections, including *Escherichia coli*, *Pseudomonas aeruginosa*, methicillin-resistant *Staphylococcus aureus*, *Candida albicans*, *Cryptococcus neoformans*, *Mycobacterium intracellulare*, and *Aspergillus fumigatus*. The antimicrobial assay was conducted in three steps (primary, secondary, and tertiary assays) in order to determine the IC_{50} and MIC values. If the compound showed no activity in the primary assay, no continuation in secondary and tertiary assays was completed. These depsipeptides do not demonstrate activity against *E. coli*, *P. aeruginosa*, or methicillin-resistant *S. aureus*. No analogues showed activity against *M. intracellulare* with the exception of **3**, which showed inhibition at an IC_{50} of 14.32 μM, while **8** inhibited at an IC_{50} of 11.98 μM (Table 2). These data revealed that introduction of a thienylmethyl substitute to the primary amine and acetylation of the secondary alcohol of kahalalide F alter the spectrum of antibacterial activity. Results revealed that modification of the primary amine with thienylmethyl led to improved activity against *M. intracellulare* compared to acetylation products.

Interestingly, **1** and its analogues exhibited significant activity against a fungus type yeast (*C. albicans*), dimorphic fungus (*C. neoformans*), and filamentous fungi (*A. fumigatus* and *Fusarium* spp.). The in vitro activity against fungi is shown in Table 2.

Peptide **1** as well as several analogues such as, **3**, **8**, and **10** exhibited activity against *C. albicans*, *C. neoformans*, and *A. fumigatus*. Analogues **4**, **5**, **7**, and **11** show selectivity against certain types of fungi. Analogue **4** was active against *C. albicans* and *C. neoformans*, while **7** inhibited *C. albicans*, *C. neoformans* and *A. fumigatus*. Products **5** and **11** were selective against *C. neoformans*. Kahalalide D, **2**, and analogues **6** and **16** showed no activity in the antimicrobial assays and were not subjected to further evaluation. Vero cells at 4760 ng/mL showed no significant toxicity for **1** and its analogues.

2.B. Antiparasitic Activity. 1 and its analogues were subjected to evaluation against *Plasmodium falciparum* and *Leishmania donovani*. **1** and analogues **8** and **10** were active against *Leishmania donovani* with IC_{50} and IC_{90} values of 17–19 and 34–40 μg/mL. No compounds from this class showed significant antimalarial activity against *P. falciparum* D6 clone and W2 clone.

Table 3. Minimum Inhibitory Concentration (MIC) of **1** Analogues versus *Mycobacterium tuberculosis* H37Rv Strains[a]

compd	% inhibition at 16 μg/mL	MIC (μg/mL)
RMP	93	0.08
1	67	>16
KD	49	NT
2	29	NT
3	94	15.4
5	77	NT
7	24	NT
8	92	15.5
10	88	>16
11	91	9.4
16	46	NT

[a] NT = not tested. RMP = rifampcin.

2.C. Bioactivity against *Mycobacterium tuberculosis*. 1 and its analogues were evaluated against *M. tuberculosis* strain H37Rv. All compounds were evaluated at 16 μg/mL. The MIC was determined for compounds that showed greater than 90% inhibition (Table 3). Analogues **3**, **8**, and **11** were more active than **1** and produced 91–94% inhibition, respectively, while the other analogues were determined to be inactive at 16 μg/mL. Analogue **11** showed better potency than analogues **3** and **8** against *M. tuberculosis*. In addition, analogue **11** was less active against *M. intracellulare*, a relatively nonpathogenic model organism for genus *Mycobacterium*. This activity difference between analogue **11** and analogues **3** and **8** demonstrates a selectivity of analogue **11** against *M. tuberculosis*. Overall, the findings indicated that O-acetylation of secondary alcohol or N-alkylation of primary amine can significantly improve the activity and selectivity of the parent molecule to the target.

2.D. Bioactivity against *Fusarium* spp. Our interest in the activity of **1** and its analogues against *Fusarium* spp. is inspired by the fact that a limited number of antifungal agents are effective against *Fusarium*, and **1** possesses well established antifungal activity. In addition, there is a growing need to identify drugs to alleviate opportunistic fungal infections in immunocompromised patients who become susceptible to a variety of fungal infections caused by *Fusarium* spp. Two bioassay methods have been employed to examine the activity of **1** and its analogues against *Fusarium* spp.

2.D.1. Bioautography Assay. Two bioassay methods have been employed to examine the activity of **1** and its analogues against *Fusarium* spp. Bioautography was utilized as a prelimi-

Table 4. Microtiter Analysis of Kahalalide Analogues at Different Concentrations (48 and 72 h)

compd	% inhibition[a] (0.3 μM)			% inhibition[a] (3.0 μM)			% inhibition[a] (30 μM)		
	Fusarium oxysporum	*Fusarium proliferatum*	*Fusarium solani*	*Fusarium oxysporum*	*Fusarium proliferatum*	*Fusarium solani*	*Fusarium oxysporum*	*Fusarium proliferatum*	*Fusarium solani*
1	0 (0)	0 (0)	0 (0)	0 (0)	0 (0)	9.9 (0)	100 (99.6)	99.8 (100)	98.9 (99.9)
3	0 (0)	0 (0.3)	0 (0)	0 (0)	0 (0.3)	0 (0)	78.5 (74.4)	70.8 (34.7)	80.9 (96.7)
4	1.8 (0)	1.8 (0)	0 (0)	1.8 (0)	5.0 (0)	0 (0)	91.9 (82.2)	92.7 (73.2)	90.6 (85.5)
5	0 (0)	0 (0)	0 (0)	0 (0)	0 (0)	16.5 (0)	96.6 (94.3)	97.5 (96.1)	97.3 (97.3)
7	0 (0)	0 (0)	0 (0)	0 (0)	0 (0)	0 (0)	98.2 (91.2)	99.1 (95.3)	99.2 (97.5)
8	0 (0)	0 (0)	0 (0)	13.7 (0)	4.8 (0)	47.0 (32.9)	98.8 (99.2)	98.7 (99.0)	99.0 (99.3)
10	0 (0)	0 (0)	0 (0)	0 (0)	0 (0)	0 (0)	93.6 (89.0)	95.3 (92.8)	94.3 (94.7)
16	0 (0)	0 (0)	0 (0)	0 (0)	0 (0)	0 (0)	0 (0)	0 (0)	0 (0)
azoxystrobin	22.7 (15.3)	0 (0)	16.6 (11.7)	32.3 (7.1)	21.7 (14.8)	25.3 (15.0)	77.2 (32.9)	53.0 (40.7)	62.7 (51.7)
captan	0.2 (0)	6.0 (3.0)	0 (0)	7.6 (0)	12.0 (0)	5.1 (0)	99.5 (98.1)	100 (100)	90.7 (47.9)
amphotericin B	0 (0)	0 (0)	0 (0.1)	12.5 (0)	7.9 (0)	18.1 (0)	99.7 (87.1)	99.8 (79.0)	100 (98.1)

[a] Sample results only indicate inhibition. Zero (0) does not indicate the degree of stimulation, only that there was no inhibition. Numbers above are 48 h results. Numbers enclosed in parentheses are 72 h results.

Table 5. Fungistatic (FS) and Fungicidal (FC) Activity of **1** and Its Analogues at 30 μM against *Fusarium* spp.

compd	antifungal activity at 30 μM		
	Fusarium oxysporum	*Fusarium proliferatum*	*Fusarium solani*
1	FC	FC	FC
3	FS	FC	FC
4	FC	FS	FC
5	FS	FS	FC
7	FS	FC	FC
8	FC	FS	FC
10	FS	FS	FC
16	NA	NA	NA
azoxystrobin	FS	FS	FS
captan	FS	FS	FS
amphotericin B	FC	FC	FC

nary screen to detect the antifungal activity and was followed by a microtiter assay. **1** and its analogues were found to be active against *F. proliferatum*. Modification of structure does not appear to have an affect on the interaction to specific species of *Fusarium* (Supporting Information). This data shows that oxidation of the secondary alcohol to **4** broadens the spectrum of activity against *Fusarium* spp. and that all other **1** analogues are ineffective against *F. solani* and *F. oxysporium* (Supporting Information).

2.D.2. Microtiter Assay. In contrast with bioautography data, the microtiter assay revealed that **1** and its analogues exhibit activity against *F. oxysporium, F. proliferatum*, and *F. solani* at the highest concentration tested (30 μM). Table 4 shows the percent inhibition of *Fusarium* spp. after treatment with compounds at three different concentrations for 48 and 72 h.

At the lowest concentration (0.3 μM) none of the compounds showed activity except for **4** after 48 h of exposure; however, the activity was lost after 72 h with the exception of azoxystrobin [methyl (*E*)-2-((6-(2-cyanophenoxy)-4-pyrimidinyl)oxy)-α-(methoxymethylene)benzeneacetate], which caused inhibition of *F. oxysporum* and *F. solani*.

At 3 μM, compound **5** showed 16% inhibition against *F. solani* after 48 h but no activity after 72 h. Analogue **8** inhibited all *Fusarium* spp. tested, with the highest activity against *F. solani*, which showed 47% inhibition after 48 h and decreased to 32.9% inhibition after 72 h. Amphotericin B and **1** showed 18% and 9.9% inhibition after 48 h, respectively. Analogue **4** showed inhibition against *F. oxysporum* and *F. proliferatum*. Analogue **5** revealed selectivity against *F. solani* after 48 h of exposure, but the activity was diminished at 72 h. All compounds showed no activity after 72 h at 3 μM with the exception of analogue **8** and azoxystrobin, which remained active against *F. solani*.

At the highest concentration (30 μM), all compounds except for **16** exhibited activity against *Fusarium* spp. The compounds provided better activity in comparison to azoxystrobin and captan [3a,4,7,7a-tetrahydro-2-[(trichloromethyl)thio]-1*H*-isoindole-1,3(2*H*)-dione]. Activity against *F. oxysporium* declined after 72 h of exposure in treatments with standard antifungals (amphotericin B and azoxystrobin) as well as analogues with **3**, **4**, and **10**. **1**, analogue **8**, and captan maintained their antifungal activity after 72 h. The active compounds against *F. proliferatum* showed more than 90% inhibition except for **3** and azoxystrobin. Captan, **1**, **5**, **8**, and **10** remained active against *F. proliferatum* after 72 h of exposure at 30 μM. Improved antifungal activity was observed for compound **3**, which remained active after 72 h of exposure with an inhibition of 96.7%. All active compounds were observed to be more active than azoxystrobin.

Figure 3 presents graphs of the growth response of *F. oxysporium*, *F. proliferatum*, and *F. solani* after 72 h of exposure to the compounds. Growth stimulation of fungi was observed at 0.3 and 3 μM, while inhibition was shown at 30 μM. Growth stimulation due to the presence of drug is a common phenomenon in antifungal therapy. This observation shows how antifungal therapy given in inappropriate doses will be a growth stimulator rather than inhibitor. More than 90% inhibition was observed in *F. oxysporum* and *F. proliferatum* in the presence of **1**, **5**, **7**, **8**, and **10** comparable to standards (amphotericin B and captan). All analogues except for **16** caused more than 90% inhibition of *F. solani* comparable to amphotericin B, while captan and azoxystrobin inhibited less than 50%.

2.D.3. Fungistatic and Fungicidal Activity. The fungistatic and fungicidal effect of each analogue was examined at 30 μM after 72 h using a microtiter plate assay. The solution from each well was grown on an agar plate free of drug to observe the growth of fungus. The results are shown in Table 5.

The results showed that the standard amphotericin B acts as a fungicidal agent against *Fusarium* spp. while captan and azoxystrobin are fungistatic. **1** analogues were fungicidal against *F. solani*, but **1** was consistently fungicidal against the three species of *Fusarium* tested. The analogues showed various fungicidal and fungistatic effects against *F. oxysporium* and *F. proliferatum*. From these data it suggests that modification of **1** appears to alter its mode of action against *Fusarium* spp. Unfortunately, modification of **1** with coumarin (**16**, our fluorescent probe) eliminated the antifungal activity. Our data indicated that analogues **7** and **8** show promising antifungal activity against *Fusarium* spp. with potency better than that of the gold standard (amphotericin B) for antifungal therapy (Table 4 and Figure 3). Although the full therapeutic window of these
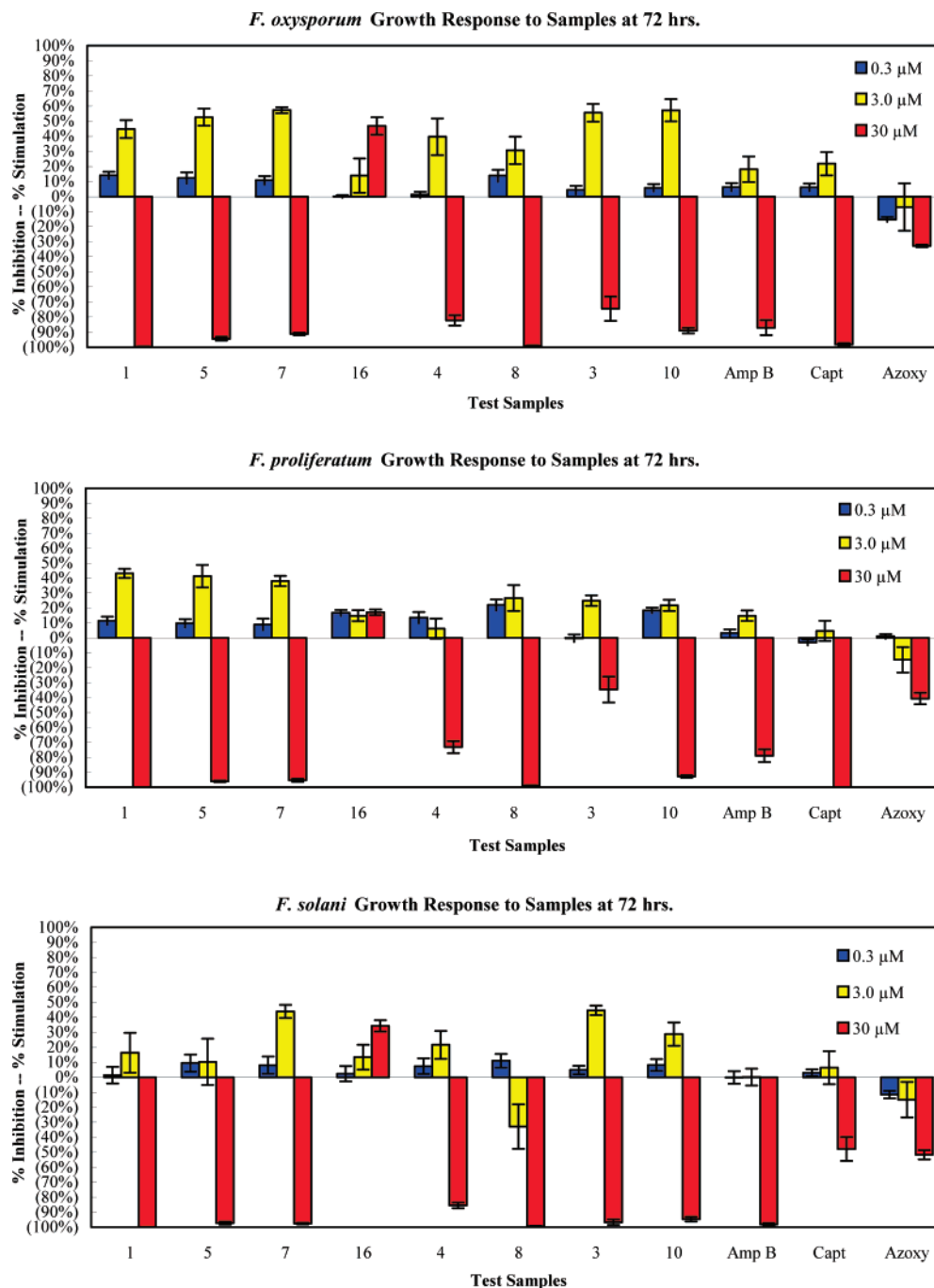
Figure 3. Growth response of *F. oxysporium*, *F. proliferatum*, and *F. solani* at three different concentrations of analogues.

1 analogues has not been addressed, their activity highlights the potential for development of **1** for antifungal therapy.

2.D.4. Fluoresence and Microscopy Analysis. In order to better understand the effect of **1** and its analogues against *Fusarium* spp., we investigated the mode of transport of the compound through the fungus. The fluorescence probe provided an excellent tool for tracking the compounds in the cell. We started by observing autofluorescence of the conidia; hyphae and mycelia resulted in no autofluorescence observation (Supporting Information). The fungus was grown in the presence of analogue **16** at 20 μg/mL. Although **16** showed no antifungal activity, it resulted in an interesting fluorescence image under fluorescence microscopy (Figure 4). The pictures generated under light and fluorescence microscopy showed the destruction and clear effect of labeled **1** against *F. proliferatum* after 3 days of exposure. Parts a and b of Figure 4 show a change of mycelia

morphology and fungal cell lysis, while parts c and d of Figure 4 show split hyphae and leakage of mycelia. All these processes can be seen very clearly under a fluorescence microscope relative to light microscope.

2.E. Cytotoxicity. Four new analogues of **1** (**5**, **7**, **8**, and **16**) were selected and evaluated for in vitro anticancer drug screening in a panel of 60 human cancer cell lines (the NCI-60) as a part of the Developmental Therapeutics Program at the National Cancer Institute (Supporting Information). These **1** analogues exhibited significant activity against selected cell lines, in particular NSCL, colon, ovarian, and breast cancers and especially prostate cancer (Table 6).

The total growth inhibition (TGI) of **1** and its analogues exhibited higher cytotoxic potency than paclitaxel against most of the human cell lines.
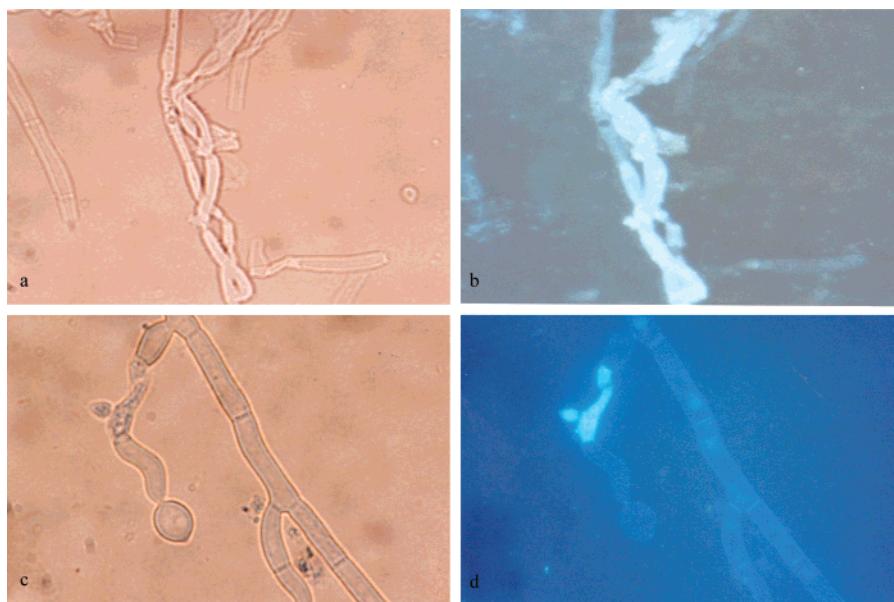
Figure 4. Mycelia of *F. proliferatum* after 3 days of exposure with fluorescent **16**: (a, c) under light microscopy (400×); (b, d) under fluorescence microscopy (400×).

Table 6. In Vitro Activity Data of Compounds **5**, **7**, **8**, and **16** (μM) against Various Cell Lines[a]

cancer	cell line	paclitaxel[b] GI_{50}	TGI	**1**[b] GI_{50}	TGI	**5** GI_{50}	TGI	**7** GI_{50}	TGI	**8** GI_{50}	TGI	**16** GI_{50}	TGI
NSCL	A549/ATCC	0.004	25.11	0.135	0.302	0.161	0.340	0.189	0.425	0.166	−	13.70	>100
	NCI-H322M	0.013	6.310	0.191	0.372	0.203	0.429	0.131	0.238	0.167	0.304	0.165	0.490
leukemia	RPMI-8226	0.002	5.012	1.738	6.918	0.475	1.780	0.638	1.890	1.270	2.760	40.10	>100
colon	COLO 205	0.003	0.316	−	−	0.156	0.315	0.618	−	0.243	−	4.520	>100
	HCC-2998	0.003	0.126	0.288	0.616	0.201	0.517	0.236	0.732	0.255	0.971	2.270	11.40
	HCT-15	0.158	15.85	0.269	0.741	0.151	0.289	0.492	1.560	0.416	1.360	0.964	17.70
	HT29	0.002	0.251	0.162	0.316	0.151	0.288	0.279	−	0.187	−	2.390	>100
	KM12	0.004	15.85	0.182	0.363	0.179	0.379	0.152	−	0.226	0.503	0.413	3.070
CNS	SNB-75	0.004	0.126	0.224	1.905	0.265	0.655	1.290	2.610	1.010	2.190	2.110	6.870
melanoma	UACC-257	0.040	25.12	1.023	2.818	1.250	0.249	1.310	2.430	1.440	2.820	> 100	>100
ovarian	SK−OV-3	0.008	15.85	0.191	0.355	0.183	0.387	0.374	1.360	0.223	0.485	2.550	20.20
renal	ACHN	0.398	12.59	1.659	3.236	1.080	2.06	1.280	2.320	1.320	2.370	26.40	69.80
prostate	PC-3	0.004	10.00	0.170	0.324	0.142	0.287	0.267	0.973	0.228	0.665	3.700	21.80
	DU-145	0.005	0.794	−	−	0.112	0.230	0.124	0.266	0.144	0.292	0.330	1.830
breast	T-47D	−	−	−	−	0.161	0.333	−	−	0.191	0.394	0.518	2.830
	HS 578T	0.003	0.100	0.162	0.479	0.212	0.695	0.162	0.444	0.427	2.130	3.030	>100

[a] Dash (−) = no data. GI_{50} (50% inhibition of cell growth): the concentration needed to reduce the growth of treated cells to half that of untreated (i.e., control) cells. TGI (100% (total) growth inhibition): the concentration required to completely halt the growth of treated cells. [b] Developmental Thrapeutics Program NCI/NIH (http://dtp.nci.nih.gov).

In particular, **5** showed better activity than **1** against RPMI-8226, HCC-2998, HT29, SK-OV-3, ACHN, and PC3 cell lines. These findings revealed highly promising improvements associated with the modification of **1**. Analogues **7**, **8**, and **16** showed better activity than **1** against NCI-H322M. Analogues **7** and **8** exhibited better potency than **1** against HCC-2998.

Analogue **5** demonstrates significant in vitro cytotoxicity against all human cancer cell lines in the panel, while amidation of **1** with coumarine (analogue **16**) resulted in the loss of activity in most cases. Derivatization of primary amine with 4-fluorobenzyl led to better activity than either 4-pyridinylmethyl or 2-thienylmethyl moieties. Compounds **5**, **7**, and **8** were shown to be nonselective in the inhibition of human cancer cell lines, while **16** had improved selectively for certain types of cell lines (NCI-322M, HCT 15, KM 12, DU-145, T-47D).

Regarding the activity against NSCL, analogues **5**, **7**, and **8** caused 50% growth inhibition at 0.161, 0.189, and 0.166 μM, respectively, for A549 while analogue **16** provided an inhibition at higher concentration (GI_{50} = 13.189 μM). In contrast, analogue **16** showed activity against NCI-H322M with a GI_{50} of 0.165 μM, comparable to analogue **8** (GI_{50} = 0.167 μM)

and better than **5** (GI_{50} = 0.203 μM). These data indicated the selectivity of **16** against different types of NSCL cell lines. The same phenomenon was observed in the activity against prostate, breast, and colon cancer cell lines. Analogues **5**, **7**, and **8** showed potent in vitro cytotoxic activity against a panel of human prostate and breast cancer cell lines, with a GI_{50} ranging from 0.112 μM (DU-145) to 0.427 μM (HS 578T). Analogue **16** exhibited activity against prostate cell line type DU-145 with a GI_{50} of 0.330 μM and against breast cancer cell line type T-47D with a GI_{50} of 0.518 μM.

In summary, this work represents the first solution-phase semisynthetic modification and lead-exploration study of **1**. This is also the first optimization of **1** as an antifungal agent against filamentous fungi of the genus *Fusarium*. These limited lead exploration studies led to the discovery of new analogues of **1** with significant in vitro improvements against selected cancer cell lines and fungi compared to the parent molecule.

Experimental Section

General Experimental Procedures. The ^{1}H and ^{13}C NMR spectra were recorded in DMSO-d_6 and MeOD on a Bruker DRX

NMR spectrometer operating at 400 MHz for ^{1}H and at 100 MHz for ^{13}C NMR. Chemical shift (δ) values are expressed in parts per million (ppm) and are referenced to the residual solvent signals of DMSO-d_6 and MeOD at δ_H/δ_C 2.50/39.5 and 3.31,4.78/49.1, respectively. UV and IR spectra were respectively obtained using a Perkin-Elmer Lambda 3B UV/vis spectrophotometer and an AATI Mattson Genesis series FTIR instrument. Optical rotations were measured with a JASCO DIP-310 digital polarimeter. The high-resolution ESI-MS spectra were measured using a Bruker Daltonic (GmbH, Germany) micro-TOF series with electrospray ionization. TLC analysis was carried out on precoated silica gel G$_{254}$ aluminum plates.

Chemicals. Kahalalide F was prepared according to the previously reported methods with some modifications.[1] The animals (*Elysia rufescens*) were collected by snorkeling at low tide near Black Point, O'ahu, in Hawaii. The ethanolic extract of freeze-dried animals was subjected to flash column chromatography on silica gel (EtOAc/MeOH). Preparative HPLC using a Phenomenex 100 mm RP C8 column (250 mm × 100 mm) and a gradient MeCN (0.05% TFA)/H$_2$O followed by further HPLC purification on an amino column (250 mm × 22 mm) using gradient EtOAc/MeOH afforded **1** as a white amorphous powder. All reagents and solvents were obtained from commercial vendors and were utilized without further purification.

Kahalalide G (2). A solution of kahalalide F free base (30 mg, 20 μmol) and potassium carbonate (0.2 g) in H$_2$O/MeOH (1:2) (10 mL) was stirred at room temperature for 8 h. The mixture was partitioned between CHCl$_3$/IPA (2:1) and water. The organic layer was dried over Na$_2$SO$_4$, and the solvent was evaporated under reduced pressure. Reversed-phase HPLC using gradient MeCN (0.05% TFA)/water afforded 28.4 mg (95%) of **2** as a white powder.[2] Yield 95.0%; $[\alpha]^{25}_D$ −12.3° (*c* 0.20, MeOH); UV λ_{max} (MeOH) 195 nm; IR neat (NaCl) 3281 (s, br), 2966 (s), 2937 (s), 1732 (s), 1636 (s),1541 (s), 1456 (s), 1204 (s), 1139 (s) cm^{-1}; HRESIMS *m/z* calcd for C$_{75}$H$_{127}$N$_{14}$O$_{17}$ [M + H]$^+$ 1519.9498, found 1519.9466.

Monoacetylated-KF (3). To a suspension of kahalalide F free base (30 mg, 20 μmol) in anhydrous dichloromethane (5 mL) were added acetic anhydride (0.4 mL) and boron trifluoride−diethyl etherate (0.2 mL) at room temperature under a nitrogen atmosphere. The mixture was stirred for 5 min, poured into a cool saturated NaHCO$_3$ solution (20 mL), and extracted with CHCl$_3$/IPA (2:1) (2 × 10 mL). The combined organic layers were dried over Na$_2$SO$_4$, and the solvent was evaporated under reduced pressure. The purification was carried out with HPLC using a Phenomenex Luna RP C8 column (250 mm × 22 mm) eluted with a gradient water/MeCN (0.05% TFA) to give 20.7 mg (68%) of **3**. Yield 68.0%; $[\alpha]^{25}_D$ −10.5° (*c* 0.25, MeOH); UV λ_{max} (MeOH) 194, 222 nm; IR neat (NaCl) 3283 (s, br), 2967 (s), 2936 (s), 1735 (s), 1654 (s),-1458 (s), 1389 (s), 1140 (s) cm^{-1}; HRESIMS *m/z* calcd for C$_{77}$H$_{127}$N$_{14}$O$_{17}$ [M + H]$^+$ 1519.9498, found 1519.9478.

Oxo-KF (4). To a solution of Dess−Martin periodinane (22 mg, 48 μmol) in anhydrous acetonitrile (10 mL) was added kahalalide F (60 mg, 40 μmol) in one portion, and the mixture was stirred at room temperature for 1 h under nitrogen atmosphere. The reaction mixture was quenched with 10% Na$_2$S$_2$O$_3$/saturated aqueous NaHCO$_3$ (v/v 1:1, 20 mL) and extracted with CHCl$_3$/IPA (2:1) (2 × 20 mL). The combined organic layers were dried over Na$_2$SO$_4$, and the solvents were evaporated under reduced pressure. The residue was subjected to preparative HPLC using a Phenomenex Luna RP C8 column (250 mm × 22 mm) eluted with gradient water/MeCN (0.05% TFA) to afford 44.2 mg (75%) of pure oxidized compound **4** as a white powder. Yield 75.0%; $[\alpha]^{25}_D$ −5.4° (*c* 0.10, MeOH); UV λ_{max} (MeOH) 195 nm; IR neat (NaCl) 3319 (s, br), 2961 (s), 2925 (s), 1731 (s), 1645 (s), 1531 (s), 1455 (s), 1392 (s) cm^{-1}; HRESIMS *m/z* calcd for C$_{75}$H$_{123}$N$_{14}$O$_{16}$ [M + H]$^+$ 1475.9236, found 1475.9237.

General Preparation of Compounds 5−11. To a solution of kahalalide F (29.5 mg, 20 μmol) and aldehyde in anhydrous methanol (5 mL) were added 3 Å molecular sieves (2 g), and the mixture was stirred for 30 min at room temperature under argon

followed by portionwise addition of sodium triacetoxyborohydride (8.5 mg, 40 μmol) over a 20 min period. The reaction mixture was stirred for period of time described below, quenched with water (20 mL), and extracted with IPA/CHCl$_3$ (1:2) (2 × 10 mL). The combined organic layers were dried over anhydrous Na$_2$SO$_4$, and the solvent was removed under vacuum. The resulting residue was purified with preparative HPLC using a Phenomenex Luna RP C8 column (250 mm × 22 mm) and eluted with gradient MeCN (0.05% TFA)/water to yield the corresponding monoalkyl-KF (major) and dialkyl-KF (minor) products as colorless powders.

4-Fluorobenzylamino-KF (5). Starting material 4-fluorobenzaldehyde (10.6 μL, 100 μmol) was used, and the reaction mixture was stirred for 18 h. Yield 64.5%; $[\alpha]^{25}_D$ −11.9° (*c* 0.25, MeOH); UV λ_{max} (MeOH) 196 nm; IR neat (NaCl) 3281 (s, br), 2966 (s), 2935 (s), 1774 (s), 1655 (s), 1538 (s), 1450 (s), 1204 (s) cm^{-1}; HRESIMS *m/z* calcd for C$_{82}$H$_{130}$FN$_{14}$O$_{16}$ [M + H]$^+$ 1585.9768, found 1585.9769.

Bis(4-fluorobenzyl)amino-KF (6). Yield 3.1%; HRESIMS *m/z* calcd for C$_{89}$H$_{134}$F$_2$N$_{14}$O$_{16}$ [M + H]$^+$ 1694.0148, found 1694.0140.

4-Pyridinylmethylamino-KF (7). Starting material 4-pyridinecarboxaldehyde (9.5 μL, 100 μmol) was used, and the reaction mixture was stirred for 2 days. The preliminary stirring of the reaction mixture for 30 min was not completed. Yield 53.1%; $[\alpha]^{25}_D$ −9.1° (*c* 0.19, MeOH); UV λ_{max} (MeOH) 193 nm; IR neat (NaCl) 3281 (s, br), 2965 (s), 2923 (s), 1741 (s), 1647 (s), 1541 (s), 1523 (s), 1457 (s), 1203 (s), 1139 (s) cm^{-1}; HRESIMS *m/z* calcd for C$_{81}$H$_{130}$N$_{15}$O$_{16}$ [M + H]$^+$ 1568.9815, found 1568.9814.

2-Thienylmethylamino-KF (8). Starting material 2-thiophenecarboxaldehyde (9.2 μL, 100 μmol) was used, and the reaction mixture was stirred for 3 days. Yield 52.3%; $[\alpha]^{25}_D$ −8.0° (*c* 0.25, MeOH); UV λ_{max} (MeOH) 193 nm; IR neat (NaCl) 3283 (s, br), 2966 (s), 2936 (s), 1734 (s), 1648 (s), 1541 (s), 1524 (s), 1458 (s), 1203 (s) cm^{-1}; HRESIMS *m/z* calcd for C$_{80}$H$_{129}$N$_{14}$O$_{16}$S [M + H]$^+$ 1573.9426, found 1573.9429.

Bis(2-thienylmethyl)amino-KF (9). Yield 12.6%; HRESIMS *m/z* calcd for C$_{85}$H$_{133}$N$_{14}$O$_{16}$S$_2$ [M + H]$^+$ 1669.9465, found 1669.9461.

***n*-Hexylamino-KF (10).** Starting material *n*-hexanal (12.3 μL, 100 μmol) was used, and the reaction mixture was stirred for 1 h. Yield 45.1%; $[\alpha]^{25}_D$ −7.2° (*c* 0.10, MeOH); UV λ_{max} (MeOH) 195 nm; IR neat (NaCl) 3280 (s, br), 2964 (s), 2934 (s), 1732 (s), 1651 (s), 1539 (s), 1456 (s), 1203 (s) cm^{-1}; HRESIMS *m/z* calcd for C$_{81}$H$_{137}$N$_{14}$O$_{16}$ [M + H]$^+$ 1562.0331, found 1562.0334.

Di-*n*-hexylamino-KF (11). Yield 25.3%; $[\alpha]^{25}_D$ −18.2° (*c* 0.25, MeOH); UV λ_{max} (MeOH) 195 nm; IR neat (NaCl) 3282 (s, br), 2964 (s), 2935 (s), 1732 (s), 1646 (s), 1540 (s), 1457 (s), 1204 (s), 1137 (s) cm^{-1}; HRESIMS *m/z* calcd for C$_{87}$H$_{149}$N$_{14}$O$_{16}$ [M + H]$^+$ 1646.1270, found 1646.1271.

DEAC-KF-amide (16). 7-Diethylaminocoumarin-3-carboxylic acid (5.3 mg, 20.3 μmol), HBTU [*O*-(benzotriazol-1-yl)-*N*,*N*,*N'*,*N'*-tetramethyluronium hexafluorophosphate] (9.2 mg, 24.4 μmol), and EDC [*N*-ethyl-*N'*-(3-dimethylaminopropyl)carbodiimide] (4.3 μL, 24.4 μmol) were dissolved in anhydrous DMF (5 mL). A solution of kahalalide F (30.0 mg, 20.3 μmol) in anhydrous DMF (2 mL) was added portionwise over 10 min at 0 °C, followed by stirring for 1 h at room temperature. The reaction was quenched by adding water (10 mL) followed by extraction with IPA/CHCl$_3$ (1:2) (2 × 10 mL). The combined organic layers were dried over anhydrous Na$_2$SO$_4$, and the solvent was evaporated under reduced pressure. The resulting residue was purified with HPLC using a Phenomenex Luna RP C8 column (250 mm × 22 mm) and eluted with gradient MeCN (0.05% TFA)/water to afford **16** as a white powder. Yield 84.9%; $[\alpha]^{25}_D$ −9.1° (*c* 0.20, MeOH); UV λ_{max} (MeOH) 201, 422 nm; IR neat (NaCl) 3319 (s, br), 2959 (s), 2924 (s), 1731 (s), 1644 (s), 1514 (s), 1455 (s), 1233 (s), 1135 (s) cm^{-1}; HRESIMS *m/z* calcd for C$_{89}$H$_{138}$N$_{15}$O$_{19}$ [M + H]$^+$ 1721.0287, found 1721.0282.

Pathogen Production of *Fusarium*. *F. solani* (F-0007), *F. oxysporium* (F-0001), and *F. proliferatum* (F0029-1) were obtained from USDA-ARS Laboratory, Natural Products Utilization Research Unit, National Center for Natural Products Research, The University

of Mississippi. The isolates were isolated from orchid species by D. E. Wedge and identified by Dr. W. H. Elmer, Connecticut Agricultural Experiment Station. The cultures were stored on silica gel in the USDA-NPURU repository. The isolates were found to be pathogenic to orchid species. *Fusarium* spp. cultures were initiated on potato dextrose agar (PDA, Difco, Detroit, MI) from spores. Conidia were harvested from 7 day old culture by flooding plates with 10 mL of sterile distilled water and dislodging using an L-shape glass rod. Conidial suspensions were filtered through sterile Miracloth (Calbiochem-Novabiochem Corp., La Jolla, CA) to remove mycelia. Concentration of conidia was determined photometrically at 625 nm from a standard curve. The concentration of conidia was 3×10^5 conidia/mL. The conidia suspension was used for one-dimensional direct bioautography and other experiments.

Bioautography Assay. Each compound was dissolved in methanol at 1 mg/mL. An amount of 100 μL of compounds was spotted on a glass thin layer chromatography plate (TLC plate, silica gel GF, 250 μm, 10 cm $\times$ 20 cm, Uniplate, Analtech, Inc., Newark, DE) and allowed to dry. The initial concentration of each compound tested was 100 μg/mL. After drying, the plates were sprayed with spore suspensions of *Fusarium* spp. Conidial solution was prepared with potato dextrose broth 12 g/500 mL, 0.1% bacto agar, and 0.1% Tween-80 and contained 3×10^5 conidia/mL of each *Fusarium* spp. Plates were placed in a moisture chamber (Pioneer Plastic, Inc., Dixon, KY) and incubated for 3 days at 26 °C. After incubation, plates were removed from the moisture chamber, dried at room temperature, and exhaustively sprayed with 0.25% MTT (3-(4,5-dimethylthiazl-2-yl)-2,5-diphenyltetrazolium bromide, Sigma) prepared in phosphate buffer. The plates were placed back into a moisture chamber and incubated at 26 °C for 1 day and allowed to develop. The active compounds were visualized by clear zones of fungal growth inhibition on TLC plates with purple background. Amphotericin B, captan, benomyl, and azoxystrobin were used as positive controls to evaluate the activity of **1** and its analogues.

Microtiter Assay. 1 and its analogues were evaluated for a dose response effect against fungi using a 96-well microdilution broth assay (Nunc, Micro Well, Roskilde, Denmark) at 0.3, 3, and 30 μM against *F. proliferatum*, *F. solani*, and *F. oxysporium* according to the procedure published by Wedge et al.[36] Microtiter plates were covered with plastic lids and incubated in a growth chamber at 24 $\pm$ 1 °C and 12 h photoperiod under 60 ± 5 μmol m^{-2} s^{-1}. Fungal growth was monitored photometrically by measuring absorbance at 620 nm at 24, 48, and 72 h. Mean absorbance values and standard error were used to evaluate fungal growth.

Fungicidal and Fungistatic Testing. The fungicidal or fungistatic assay was conducted to determine the action of each compound at 30 μM. After 72 h of incubation in a microtiter assay, 20 μL of solution of each well was cultured onto a 90 mm Petri plate containing 10 mL of potato dextrose agar free of **1** and its analogues. The plates were incubated at 28 °C for 3 days. The fungicidal effect was defined if no fungal growth was observed on the subcultured plate free of compounds, and the fungistatic activity was defined if fungal growth was observed on the subcultured plate.

Fluoresence Assay. In order to observe the effect of **1** and its analogues on *Fusarium* spp., we tested our fluorescence probe against the fungi. In a 20 mL test tube containing potato dextrose broth and conidia of *Fusarium* spp. the fluorescence compound was added at 20 μg/mL. The culture was then incubated at 24 $\pm$ 1 °C. The microscopic observation was initiated at 4, 8, 16, and 24 h and continued at 48 and 72 h. Photomicrographs of hyphae or mycelia were taken with an Olympus BX-51 microscope equipped with epifluoresence. Pictures were taken at 400$\times$ and 1000$\times$ magnification.

Mycobacterium Tuberculosis Assay. In vitro evaluation of antimycobacterial activity was conducted with *Mycobacterium tuberculosis* H37Rv ATCC 27294 in BACTEC 12B medium using microplate Alamar blue assay (MABA). Primary screening is evaluated at 16 μg/mL. Compounds that showed inhibition less than 90% were not tested further. Compounds that show inhibition of greater than 90% are retested at a lower concentration to determine the MIC values.[37]

Supporting Information Available: Spectroscopic data for **1** and its analogues; activity data of 60 NCI cell lines for compounds **5**, **7**, **8**, and **16**; fluorescence images of DEAC-carboxylic acid as a control; and bioautogram images of analogues **3**, **4**, and **5**. This material is available free of charge via the Internet at http://pubs.acs.org.

References

(1) Hamann, M. T.; Scheuer, P. J. Kahalalide F: a bioactive depsipeptide from the sacoglossan mollusk *Elysia rufescens* and the green alga *Bryopsis* sp. *J. Am. Chem. Soc.* **1993**, *115*, 5825−5826.

(2) Hamann, M. T.; Otto, C. S.; Scheuer, P. J.; Dunbar, D. C. Kahalalides: bioactive peptides from a marine mollusk *Elysia rufescens* and its algal diet *Bryopsis* sp. *J. Org. Chem.* **1996**, *61*, 6594−6600.

(3) Goetz, G.; Nakao, Y.; Scheuer, P. J. Two acyclic kahalalides from the sacoglossan mollusk *Elysia rufescens*. *J. Nat. Prod.* **1997**, *60*, 562−567.

(4) Horgen, F. D.; de los Santos, D. B.; Goetz, G.; Sakamoto, B.; Kan, Y.; Nagai, H.; Scheuer, P. J. A new depsipeptide from the sacoglossan mollusk *Elysia ornata* and the green alga *Bryopsis* species. *J. Nat. Prod.* **2000**, *63*, 152−154.

(5) Hill, R. T.; Hamann, M. T.; Enticknap, J.; Rao, K. V. Kahalalide-producing bacteria. PCT Int. Appl. WO 2005/042720, 2005.

(6) Dmitrenok, A.; Iwashita, T.; Nakajima, T.; Sakamoto, B.; Namikoshi, M.; Nagai, H. New cyclic depsipeptides from the green alga *Bryopsis* species; application of a carboxypeptidase hydrolysis reaction to the structure determination. *Tetrahedron* **2006**, *62*, 1301−1308.

(7) Ashour, M.; Edrada, R.; Ebel, R.; Wray, V.; Wätjen, W.; Padmakumar, K.; Müller, W. E. G.; Lin, W. H.; Proksch, P. Kahalalide derivatives from the Indian sacoglossan mollusk *Elysia grandifolia*. *J. Nat. Prod.* **2006**, *69*, 1547−1553.

(8) Tilvi, S.; Naik C. G. Tandem mass spectroscopy of kahalalides: identification of two new cyclic depsipeptides, kahalalide R and S from *Elysia grandifolia*. *J. Mass Spectrom.* **2006**, *42*, 70−80.

(9) Bonnard, I.; Manzanares, I.; Rinehart, K. L. Stereochemistry of kahalalide F. *J. Nat. Prod.* **2003**, *66*, 1466−1470.

(10) Lopez-Macia, A.; Jimenez, J. C.; Royo, M.; Giralt, E.; Albericio, F. Synthesis and structure determination of kahalalide F. *J. Am. Chem. Soc.* **2001**, *123*, 11398−11401.

(11) Rademaker, J. M.; Horenblas, S.; Meinhardt, W.; Stokvis, E.; de Reijke, T. M.; Jimeno, J. M.; Lopez-Lazaro, S.; Lopez, Martin, J. A.; Beijnen, J. H.; Schellens, J. H. M. Phase I clinical and pharmacokinetic study of kahalalide F in patients with advanced androgen refractory prostate cancer. *Clin. Cancer Res.* **2005**, *11*, 1854−1862.

(12) Hamann, M. T. Technology evaluation: kahalalide F (PharmaMar). *Curr. Opin. Mol. Ther.* **2004**, *6*, 657−665.

(13) PharmaMar Biopharmaceutical Co. (www.pharmamar.com). Presented at the 31st European Society for Medical Oncology Congress (ESMO), Istanbul, Turkey, September 29 through October 3, 2006.

(14) Garcia-Rocha, M.; Bonay, P.; Avila, J. The antitumoral compound kahalalide facts on cell lysosomes. *Cancer Lett.* **1996**, *99*, 43−50.

(15) Suarez, Y.; Gonzalez, L.; Cuadrado, A.; Berciano, M.; Lafarga, M.; Munoz, A. Kahalalide F, a new marine-derived compound, induces oncosis in human prostate and breast cancer cells. *Mol. Cancer Ther.* **2003**, *2*, 863−872.

(16) Faircloth, G. T.; Smith, B.; Grant, W.; Jimeno, J. M.; Garcia-Gravalos, L.; Scotto, K.; Shtil, A. Selective antitumor activity of kahalalide F, a marine-derived cyclic depsipeptide. *Proc. Am. Assoc. Cancer Res.* **2001**, *42*, 213.

(17) Janmaat, M.; Rodriguez, J.; Jimeno, J.; Kruyt, F.; Giaccone, G. Kahalalide F induces necrosis-like cell death that involves depletion of ErbB3 and inhibition of Akt signaling. *Mol. Pharmacol.* **2005**, *68*, 502−510.

(18) Jimeno, J.; Aracil, M.; Tercero, J. Adding pharmacogenomics to the development of new marine-derived anticancer agents. *J. Transl. Med.* **2006**, *4*, 1−9.

(19) (a) Jarvis, L. M. Battling breast cancer by targeting multiple HER-family receptors, small-molecule drugs could fill the therapeutic gaps left by Herceptin. *Chem. Eng. News* **2006**, *84* (32), 21−27. (b) Holbro, T.; Beerli, R. R.; Maurer, F.; Koziczak, M.; Barbas, C. F.; Hynes, N. E. The ErbB2/ErbB3 heterodimer functions as an oncogenic unit: ErbB2 requires ErbB3 to drive breast tumor cell proliferation. *Proc. Natl. Acad. Sci. U.S.A.* **2003**, *100* (15), 8933−8938.

(20) Albericio, P. F.; Giralt, L. E.; Jiménez, G. J.-C.; Lopez, M. A.; Manzanares, I.; Rodrigues, I.; Royo, E. M. Kahalalide compounds. PCT Int. Appl. WO 01/58934, 2001.

(21) Albericio, P. F.; Fernandez, D. A.; Giralt, L. E.; Gracia, C. C.; Lopez, R. P.; Varon, C. S.; Cuevas, M. C.; Lopez, M. A.; Francesca, S. A.; Jiménez, G. J.-C.; Royo, E. M. New antitumoral compounds. PCT Int. Appl. WO 2005/023846, 2005.

(22) Gracia, C.; Isidro-Llobet, A.; Cruz, L. J.; Acosta, G. A.; Alvarez, M.; Cuevas, C.; Giralt, E.; Albericio, F. Convergent approaches for the synthesis of the antitumoral peptide, kahalalide F. Study of orthogonal protecting groups. *J. Org. Chem.* **2006**, *71*, 7196−7204.

(23) Faircloth, G. T.; Elices, M.; Sasak, H.; Aviles Marin, P. M.; Cuevas Marchante, M. D. C. Preparation of kahalalide antitumoral compounds. PCT Int. Appl. WO 2004/035613, 2004.

(24) Peng, J.; Shen, X.; El Sayed, K. A.; Dunbar, D. C.; Perry, T. L.; Wilkins, S. P.; Hamann, M. T.; Bobzin, S.; Huesing, J.; Camp, R.; Prinsen, M.; Krupa, D.; Wideman, M. A. Marine natural products as prototype agrochemical agents. *J. Agric. Food Chem.* **2003**, *51*, 2246−2252.

(25) Scheuer, P. J.; Hamann, M. T.; Gravalos, D. G. Cytotoxic and antimicrobial activities of kahalalide F from *Elysia rufescens*. U.S. Patent 6274551, 2001.

(26) (a) Patai, S. *The Chemistry of Amino, Nitroso, Nitro and Related Groups*; Wiley: New York, 1996. (b) Salvatore, R. N.; Yoon, C. H.; Jung, K. W. Synthesis of secondary amines. *Tetrahedron* **2001**, *57*, 7785−7811. (c) Insaf, S. S.; Witiak, D. T. Facile non-racemizing route for the N-alkylation of hindered secondary amines. *Synthesis* **1999**, *3*, 435.

(27) Arikan, S.; Rex, J. H. New agents for the treatment of systemic fungal infections−current status. *Expert Opin. Emerging Drugs* **2002**, *7*, 3−32.

(28) De Lucca, A. J. Antifungal peptides: potential candidates for the treatment of fungal infections. *Expert Opin. Invest. Drugs* **2000**, *9*, 273−299.

(29) Hancock, R. E. W.; Chapple, D. S. Peptide antibiotics. *Antimicrob. Agents Chemother.* **1999**, *43*, 1317−1323.

(30) Vanden Bossche, H. Echinocandins, an update. *Expert Opin. Ther. Pat.* **2002**, *12*, 151−167.

(31) Martinez-Pascual, R.; Vinas-Bravo, O.; Meza-reyes, S.; Iglesias-Arteaga, M. A.; Sandoval-Ramirez, J. A fast and convenient procedure for the acetylation of alcohols. *Synth. Commun.* **2004**, *34*, 4591−4596.

(32) Meyer, S. D.; Schreiber, S. L. Acceleration of the Dess−Martin oxidation by water. *J. Org. Chem.* **1994**, *59*, 7549−7552.

(33) (a) Borch, R. F.; Bernstein, M. D.; Durst, H. D. Cyanohydridoborate anion as a selective reducing agent. *J. Am. Chem. Soc.* **1971**, *93*, 2897−2904. (b) Bomann, M. D.; Guch, I. C.; DiMare, M. A mild, pyridine-borane-based reductive amination protocol. *J. Org. Chem.* **1996**, *60*, 5995−5996. (c) Szardenings, A. K.; Burkoth, T. S.; Look, G. C.; Campbell, D. A. A reductive alkylation procedure applicable to both solution- and solid-phase syntheses of secondary amines. *J. Org. Chem.* **1996**, *61*, 6720−6722.

(34) (a) Gribble, G. W.; Ferguson, D. C. Reactions of sodium borohydride in acidic media. Selective reduction of aldehydes with sodium triacetoxyborohydride. *J. Chem. Soc., Chem. Commun.* **1975**, 535−536. (b) Nutaitis, C. F.; Gribble, G. W. Chemoselective reduction of aldehydes with tetra-*n*-butylammonium triacetoxyborohydride. *Tetrahedron Lett.* **1983**, *24*, 4287. (c) Gribble, G. W. *Encyclopedia of Reagents for Organic Synthesis*; Paquette, L. A., Ed.; John Wiley and Sons: New York, 1995; Vol. 7, p 4649.

(35) Sandler, J. S.; Fenical, W.; Gulledge, B. M.; Chamberlin, A. R.; La Clair, J. J. Fluorescent profiling of natural product producers. *J. Am. Chem. Soc.* **2005**, *127*, 9320−9321.

(36) Wedge, D. E.; Kuhajek, J. M. A microbioassay for fungicide discovery. *SAAS Bull. Biochem. Biotechnol.* **1998**, *11*, 1−7.

(37) Collins, L.; Franzblau, S. G. Microplate Alamar blue assay versus BACTEC 460 system for high-throughput screening of compounds against *Mycobacterium tuberculosis* and *Mycobacterium avium*. *Antimicrob. Agents Chemother.* **1997**, *41*, 1004−1009.